Journal of Optoelectronics and Advanced Materials Vol. 7, No. 5, October 2005, p. 2571 - 2580

Invited paper

PHOTOINDUCED DEFORMATIONS IN CHALCOGENIDE GLASSES: SCALAR AND VECTORAL[♣]

K. Tanaka[*]

Department of Applied Physics, Graduate School of Engineering, Hokkaido
University, Sapporo 060-8628, Japan

Chalcogenide glasses such as As_2S_3 and $AgAsS_2$ are known to exhibit photoinduced isotropic and anisotropic deformations. In As_2S_3, which is assumed to have segmental layer structures, the deformations are produced by interlayer-type expansive force and photoinduced fluidity. The anisotropic deformation upon illumination of linearly-polarized light arises from layer alignment. In $AgAsS_2$, photoinduced Ag^+ ion migration is responsible, which is affected by light scattering and optical interference in the anisotropic pattern formation.

(Received August 24, 2005; accepted September 22, 2005)

Keywords: Photoinduced phenomena, Photographic reaction, Weigert effect, Chalcogenide glass

1. Introduction

This year, 2005, we are celebrating the centennial anniversary of modern physics. As is well-known, in 1905, Einstein proposed the concept of “photon”, which triggered a new scientific paradigm of quantum mechanics.

Since that era, the solid state science has made a remarkable progress, in which one of the most extensively-studied materials is an ionic crystal. The material such as NaCl can easily be obtained as transparent single crystals so that fundamental studies on color-centers and so forth have attracted considerable interest. On the other hand, from application points-of-view, photographic reaction in Ag-halides posed a big problem, which should be understood for producing high-sensitive films. Results on these pioneering studies are described in the famous book by Mott and Gurney [1]. We also know that color-center formation and the photographic reaction can be affected by the direction of electric fields of excitation light [2-5].

Table 1. Comparison of photoinduced phenomena in ionic crystals and chalcogenide glasses.

Material	Photo-electro-atomic	Photo-electro-ionic
Ionic crystal	Color-center formation in alkali halide	Photographic reaction in Ag halide (Weigert effect)
Chalcogenide glass	Photoinduced phenomena in $As_2S(Se)_3$	Ag-ion migration in Ag-As(Ge)-S

[♣] paper presented at 3rd International Symposium on irradiation phenomena in chalcogenide, oxide and organic thin films, Tryavna, Bulgaria, June 15-19, 2005.

[*] Corresponding author: keiji@eng.hokudai.ac.jp

It may be a surprise, as listed in Table 1, that resembling situations and probably more prominent phenomena can be pointed out for chalcogenide glasses [6,7]. In covalent compositions such as As_2S_3, we know photoinduced optical and volume changes, which may be similar in some points to radiation-induced color-center formation in alkali halides. In Ag-chalcogenides such as $AgAsS_2$, photoinduced Ag-migration phenomena appear, which can be regarded as kinds of photographic processes [8]. Note that these changes can be scalar and vectoral, or isotropic and anisotropic, with respect to the electric field of excitation light. It should also be emphasized that some of these changes appear as big deformations, which may be noticed even by naked eyes.

Why can photons, which are mass-less quanta, produce such macroscopic deformations in these glasses? This work provides a brief review on the present understanding of the photoinduced deformation, with some new data and speculations. As typical examples, we will mostly focus upon As_2S_3 and $AgAsS_2$ glasses, including annealed films, the Tauc gaps being known as 2.4 and 2.1 eV [8]. It is mentioned here that as-evaporated films may show similar phenomena, but probably through different mechanisms [7,9-12].

2. Covalent glass As_2S_3

2.1. Historical

Situations in As_2S_3 appear to be complicated, probably due to extensive studies. The early studies of interest here, however, can be grouped into two historical flows, which may be regarded as nearly independent with each other until 1997.

One research flow is on the photoinduced volume change, which has been discovered by Hamanaka et al. [13]. For instance, when As_2S_3 is exposed to bandgap illumination ($\hbar\omega \geq 2.4$ eV) at room temperature, it undergoes a volume expansion of 0.4 %, the actual height being ~10 nm due to limited penetration depths of bandgap light [13]. Later, Hisakuni and Tanaka have found that the expansion can seemingly be enhanced to ~5 % by using sub-bandgap illumination of ~2.0 eV [14]. The enhancement factor of ten times may justify regarding this phenomenon as “giant”. The actual expansion amounts to ~2 μm [14], which is substantially greater than light wavelength, so that it can be employed for fabricating spherical and aspherical micro-lenses [15-17] and relief-type gratings [18]. Phenomenologically, the giant photoexpansion can be understood [19] with a volumetric photo-excitation effect arising from longer penetration depths of sub-gap light combined with photoinduced fluidity [20-24]. Nevertheless, it should be underlined that an intrinsic expansion at room temperature is ~0.4 %, being irrespective of the photon energy of excitation.

Volume change	*Anisotropic deformation*	*Optical anisotropy*
1976 Hamanaka et al. [13]	1997 Krecmer et al. [40]	1977 Zhdanov-Malinovsky [29]
1994 Hisakuni-Tanaka [14]		1993 Fritzsche’s model [32]
2000 Saliminia et al. [42]		

Fig. 1. Historical flows in relation to photoinduced deformations in covalent chalcogenide glasses such as As_2S_3.

Microscopic mechanism of the volume expansion remains to be controversial. Tanaka assumes that photoinduced disorder enhancement in amorphous networks combined with the photoinduced fluidity causes the photoexpansion [19,25]. This idea may resemble the Shottky-defect formation in alkali-halide crystals [1-3]. Another idea is the Coulomb repulsive model proposed by Shimakawa et al. [26,27], which has been criticized from some respects [25,28]. Both the models are largely qualitative.

The other important research flow is on photoinduced anisotropy (Fig. 1), which is believed to be discovered by Zhdanov and Malinovshii [29,30,31]. The anisotropy had been optical, i.e. dichroism and birefringence, which were *negative* in covalent chalcogenide glasses. For instance, the photoinduced birefringence Δn (= $n(//)$-$n(\perp)$, where $n(//)$ and $n(\perp)$ indicate the refractive indices parallel and perpendicular to the electric field of excitation light) in As_2S_3 exposed to linearly-polarized bandgap light at room temperature is -0.002 [30], which corresponds to ~0.1 % of the refractive index of ~2.6.

This negative anisotropy has been interpreted by Fritzsche [30,32,33]. He assumes that, in a disordered network, some anisotropic elements which align nearly in parallel to the electric field of linearly-polarized light are selectively photoexcited, and then, the element may relax to other directions. Accordingly, the polarization parallel to the electric field will decrease, which appears as the negative optical anisotropy. This concept can explain several features of the photoinduced anisotropy such as temperature dependence [30]. However, a real entity of anisotropic elements remains to be controversial, the candidate ranging from electron clouds (~0.2 nm) to segmental layers (~2 nm) [30,34]. I believe that the alignment of segmental layers, or chains in Se, is the most probable, since the model is consistent with detailed x-ray results [35,36], a close correlation between the photoinduced anisotropy and the crystalline anisotropy [35], and photoinduced oriented crystallization in amorphous Se [37-39]. Since the optical anisotropy was relatively small, we had assumed that no anisotropic deformation could be detected.

Nevertheless, Krecmer et al. [40,41] and Saliminia et al. [42] have discovered two kinds of anisotropic deformation (Fig. 1). Krecmers' discovery was made for small bilayer samples consisting of $As_{50}Se_{50}$ films and Si_3N_4 cantilevers. Bending of the bilayer sample can be controlled by changing relative directions of the electric field of linearly-polarized light to a cantilever axis. On the other hand, Saliminia et al. have found that an anisotropic pattern (see, the right profile in Fig. 2), which reflects the direction of electric fields, emerges in As_2S_3 films upon exposure to focused linearly-polarized light [42]. The group reports successive studies [43].

2.2. Deformation and birefringence

Saliminias' discovery appears to be simpler, and accordingly, we hereafter focus on this phenomenon. Then, to understand mechanisms of the polarized-light induced anisotropic deformation, we must know the relations, as indicated by the two arrows in Fig. 1, between it and both the isotropic expansion and the optical anisotropy.

Fig. 2 compares dependences of the surface deformation and the birefringence on exposure time. The sample is a 2 μm-thick annealed As_2S_3 film, which is exposed to focused linearly-polarized He-Ne laser light (2.0 eV) with intensity of 2 mW and spot diameter of ~10 μm. The surface deformation is evaluated using an atomic force microscope as a net volume change of the film from the initial flat surface. The birefringence in the illuminated region is measured using weak He-Ne laser light as in the previous study [35].

We see two interesting features. First, the expansion is initially isotropic (≤ 10 min), then the center being gradually depressed, and it grows to an anisotropic deformation [44], which is similar to that reported by Saliminia et al. [42]. A cross-sectional view of the anisotropic pattern is M-shaped, consisting of a central hollow and double-side hillocks, along the electric field of excitation light. Second, surprisingly, the negative birefringence appears with a similar time scale (~5 min) to that of the isotropic expansion, the both being much faster than a growth (~100 min) of the anisotropic deformation.

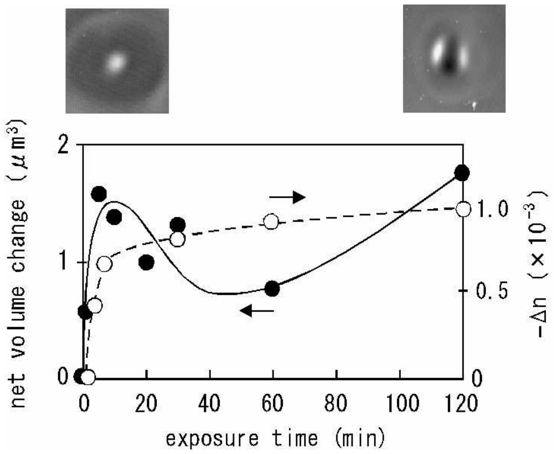

Fig. 2. Exposure-time dependence of volume change (solid circles with a solid line and the left-hand side axis) and birefringence (open circles with a dashed line and the right-hand side axis) in an As_2S_3 film. The figure includes two AFM profiles, the side lengths being 20 μm, which show an isotropic expansion at 1 min (left) and an anisotropic deformation at 60 min (right), in which the electric field of excitation light is horizontal.

2.3. Mechanism

It seems that both the isotropic and the anisotropic deformation can be understood in a coherent way with interlayer expansion (Fig. 3) and induced fluidity (Fig. 4) under illumination. In the isotropic volume expansion, as illustrated in Fig. 3, it is plausible that the interlayer disordering gives a motive force [19,25]. In the anisotropic deformation, we assume that the interlayer disordering of aligned segmental layers also gives the motive force. That is, when a segment is going to align through atomic twisting and so forth, an extra interlayer space will be needed, which produces a kind of interlayer van-der-Waals type expansive force. This atomic force combined the photoinduced fluidity can provide the macroscopic deformation. That is, in this model, the motive forces are assumed to be essentially the same in the isotropic and the anisotropic deformation, and the photo-induced fluidity is commonly responsible for the both. A difference is that the segmental layer may be crumpled in the isotropic and it is aligned in the anisotropic. On the other hand, the birefringence can be ascribed to segmental alignment in atomic scales [30,35], which may not necessarily be followed by structural relaxation through the fluidity.

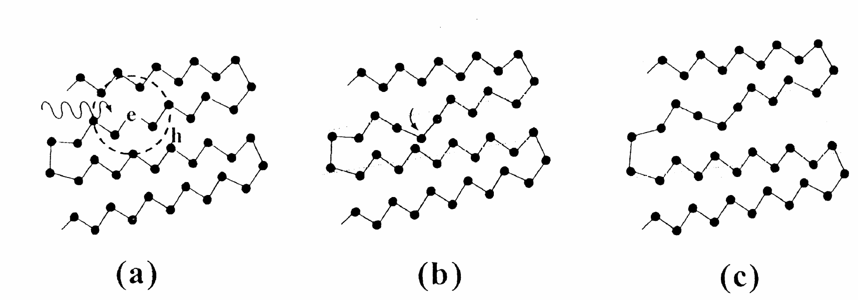

(a) (b) (c)

Fig. 3. An atomic mechanism of expansion illustrated for Se for simplicity [25]. (a) A photon excites a pair of electron and hole. (b) When relaxing, the carriers produce a bond-twisted structure, which causes inter-layer (chain) stress. (c) The stress is relaxed with inter-layer relaxation, which produces expansive stress.

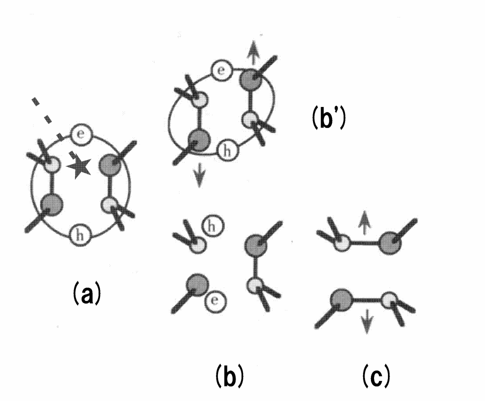

Fig. 4. An atomic mechanism of fluidity in As_2S_3. (a) A photon excites a pair of electron and hole. (b') Under the excited state, the interlayer interaction is weakened and the segments can easily flow. Otherwise, (b) the carrier produces a defect, which may relax to (c) a bond interchanged structure, and then the separated clusters can flow.

In this model, the different time scales shown in Fig. 2 can be interpreted as manifestations of the different fluidity scales. As is known, the fluidity is defined as the inverse of viscosity η, which relates shear stress $\boldsymbol{\sigma}$ and fluid velocity $\boldsymbol{u}$ (= dU/dt) as $\boldsymbol{\sigma}_z = \eta du_z/dx$, where the fluid is presumed to flow in the z direction with a velocity gradient in the x direction. In the isotropic volume expansion, as illustrated in Fig. 5(a), we can take the z direction to be perpendicular to the film surface, and the x scale is governed by the light-spot size. In the M-shaped deformation, Fig. 5(b), the z axis is parallel to the light polarization direction, and the x scale is the film thickness. Then, approximating the differential quantities with typical integrated values, we rewrite the equation as $\sigma \approx \eta U/(\tau X)$, where U is the resultant deformation, τ a response time of the viscous flow, and X the gradient scale. In a typical result for the volume expansion shown in Fig. 2, $U/X \approx 0.01\mu m/5\mu m \approx 0.002$ and$\tau \approx 300$ s, and accordingly, $\eta/\sigma \approx 10^5$ s. For the M-shaped deformation, $U/X \approx 0.05\mu m/2\mu m \approx 0.02$, in which a material expansion U has been estimated from the hillock volume, and$\tau \approx 6000$ s, which give $\eta/\sigma \approx 10^5$ s. Surprisingly, η/σ in the volume expansion and the M-shaped deformation are in similar magnitudes. Since η is assumed to be determined by the photoinduced fluidity, which is common to the both, we may take a typical value, $\eta \approx 10^{12}$ P = 10^{11} Pa·s at light intensity of 10^2 W/cm^2 [20,21]. Then, the photoinduced stress can be estimated at $\sigma = 10^6$ N/m^2 = 10^{-12} N/nm^2.

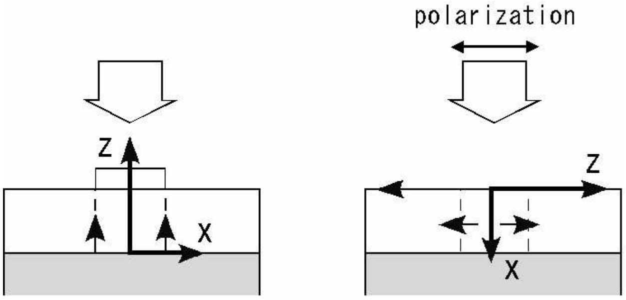

Fig. 5. Cross-sectional views of (a) the giant photoexpansion (left) and (b) the photoinduced anisotropic deformation (right). An As_2S_3 film on glass substrate is exposed to linearly-polarized light, which has the electric field, in (b), in parallel to the z axis.

This quantity appears to be comparable to interlayer atomic force. For instance, a theoretical calculation for crystalline As_2Se_3 by Tarnow et al. [45] suggests that interlayer sliding along the c-axis, which is the easiest sliding direction, by 0.2 nm needs ~10 meV/atom, which provides ~10^{-12} N/atom. On the other hand, in a hypothetical atomic plane of 1 nm^2 in $As_2S(Se)_3$ *glass*, it is plausible that only one interlayer bond, which may be as short as the crystalline value, is determinative for layer sliding. Accordingly, we can obtain 10^{-12} N/nm^2.

Such strain could arise from interlayer interaction. The photoinduced bond-twisting motion, shown in Fig. 3 [22,25,46], can cause the interaction. Otherwise, interchange of covalent bonds (Fig. 4), which is suggested as a mechanism for the photoinduced fluidity [21,33,47,48], may also produce the expansive force. In short, the motive force arising from interlayer strain and the interchange between covalent and van-der-Waals type bonds seem to be responsible for these isotropic and the anisotropic deformation.

3. Ion-conducting glass $AgAsS_2$

Ag-As-S has attracted substantial interest from two points. Initially, Borisovas' group studied its remarkable ionic conduction [6], and later, some researchers discovered photoinduced phenomena such as photodoping and photo-surface deposition [7,8,49,50]. These photoinduced phenomena can produce some surface patterns which are made from crystalline Ag. We here will focus upon the deformation emerging in amorphous structures.

Such photoinduced deformations in Ag-As-S can be divided into isotropic and anisotropic (Fig. 6) [51-54]. These deformations are the most prominent in $AgAsS_2$, which appears to be a stable composition in the Ag-As-S glass system. In contrast, Cu-As-S films do not show any deformation at all [51], which implies that the Ag ionic conduction plays an important role in the pattern formation. As is known, in electronic properties, the Cu films are similar to the Ag films [55], while the Cu system does not possess marked ionic conduction. Note that nano-scale modifications produced by a scanning tunneling microscope are also contrastive in these materials [55,56]. On the other hand, Na-Ge-S glasses, which can be regarded as an ionic (but, not ion-conducting) chalcogenide glass, also show different behaviors from those in Ag(Cu)-As-S [57].

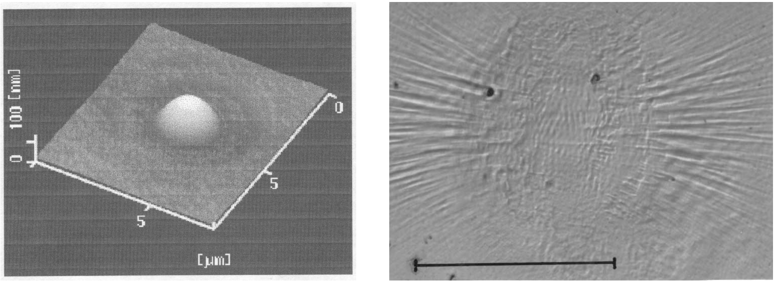

Fig. 6. Photoinduced deformations in $AgAsS_2$ films (~1 μm thick) induced with illumination of linearly-polarized He-Ne laser light. In the left-hand side deformation (a), the diameter of light spot is ~2 μm, and in the right-hand side, it is ~50 μm, which is indicated by the scale bar. In (b), the electric field is vertical.

The isotropic expansion appears when $AgAsS_2$ films are exposed to small light spots of a few micrometers in diameter [53]. In more detail, we see in Fig. 6(a) that the expansion is surrounded by a small depression. A typical exposure condition is to use light with wavelength of 633 nm (2.0 eV), which can be regarded as bandgap light, intensity of 6 kW/cm^2, and exposure time of 2 min. The expansion accompanies an Ag accumulation of ~5 at.%. Similar volume expansions appear when the film is exposed to unpolarized light and when $AgAsS_2$ bulk glasses are exposed. Or, more prominent expansions appear upon exposure of electron beams [58]. These deformations can be erased with annealing treatments at 420 K, which is the glass-transition temperature of $AgAsS_2$ [6].

The deformation mechanism can be ascribed to photo-chemical modification [8,59,60]. When the glass is illuminated, electrons and holes are photo-excited, in which only holes can diffuse in these glasses. Accordingly, the illuminated region negatively charges [61], which attracts positive Ag ions. The accumulated ions give rise to the volume expansion, which seems to be quantitatively consistent with the observations [53]. The peripheral depression corresponds probably to Ag depletion. Since the light spot is small, pattern effects described below can hardly work.

The anisotropic deformation appears when an $AgAsS_2$ film is exposed to linearly-polarized He-Ne laser light focused to a spot of ~50 μm in diameter [51,52,54]. The deformation shown in Fig. 6(b), which has been produced by an exposure of 300 W/cm^2 and 3 h, consists of two kinds of corrugations; one being small fringes in the illuminated spot which align in parallel to the electric field of light, and the other being cat-whisker like radiating patterns which are mostly perpendicular to the electric field. The fringe in the light spot diffracts transmitted light to the direction perpendicular to the fringe direction. The fringe also accompanies a *positive* birefringence Δn (= $n(//)-n(\perp)$) of ~0.01 [52]. Note that the refractive index of the film is ~3.0, so that the fractional birefringence is ~0.3 %, which is more-or-less remarkable. It has been found by using an electron-probe micro-analyzer that the fringe accompanies an Ag-composition modulation of ~5 at.%.

The deformation can be ascribed to the photo-chemical modification which occurs under unique light-intensity patterns (see, Fig. 7) [51,52,54]. We here take Mie scattering into account, which may result from dusts on the film surface, structural inhomogeneity, and so forth. As it is known, the scattering is more intense in the direction perpendicular to the electric field of light. And, the scattered light is likely to be converted to guided modes, which propagate in the film, due to the high refractive-index of the film. Then, the guided light interferes with the incident light in the light spot, and produces interference fringes. The small fringe in the light spot is assumed to be a manifestation of this fringe-induced photo-chemical modification. The fringe will work also as a grating coupler, which further intensifies the guided light. The positive birefringence can be understood to arise from this fringe structure, in which the Ag-content modulation causes the so-called form birefringence. On the other hand, the guided light may propagate toward the outside of the light spot by ~10 μm, which corresponds to the penetration depth of 2.0 eV light in this material [8]. Such light streaks may produce the cat-whisker pattern through the photo-chemical modification.

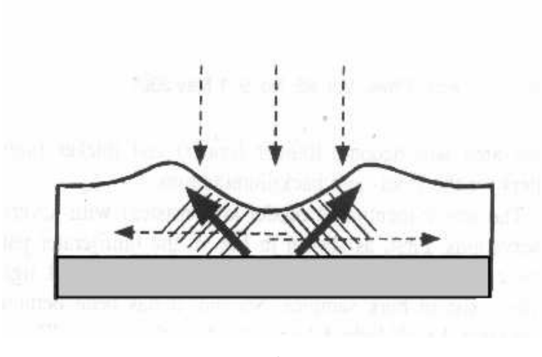

Fig. 7. A model for the anisotropic pattern formation (cross section) in an $AgAsS_2$ film exposed to linearly-polarized light spot with diameter of ~50 μm [54]. The electric field is assumed to be perpendicular to this cross-sectional view. Dashed lines with arrows represent propagation paths of incident and guided light, fringes show the interference pattern, and the two solid arrows indicate macroscopic material flow.

4. Summary

A brief review is given, with some new data and speculations, on the photoinduced deformation in chalcogenide glasses. We have seen that the phenomenon shows a great variety, which changes with exposure duration and light-spot size.

The deformation can be isotropic and anisotropic. The both types appear with the exposure duration in a covalent composition, As_2S_3, and with the light-spot size in an ion-conducting glass, $AgAsS_2$. Motive forces for the deformations are assumed to be interlayer (van-der-Waals) type in As_2S_3 and ionic in $AgAsS_2$.

In some sense, these mechanisms are reminiscent to those of the known phenomena in ionic crystals, i.e., Shottky-type color-center formation in alkali-halides and photographic reaction in Ag-halides. New aspects here are that these glasses are kinds of semiconductors, which can be excited by visible light, and photoinduced processes occur totally in amorphous structures, which may provide strong electron-lattice interaction. We can just take a leaf out of a wise man's book; in Japanese, Onko-chishin.

Finally, it should be mentioned that, experimentally, the recent progress in deformation studies is largely owe to atomic force microscopy.

Acknowledgement

I would like to thank my students, A. Saitoh, N. Yamamura, and H. Asao for experiments on As_2S_3.

References

[1] N. F. Mott, R. W. Gurney, Electronic Processes in Ionic Crystals, Dover (1964).
[2] S. V. Pappu, Contemp. Phys. **26,** 479 (1985).
[3] N. Itoh, A. M. Stoneham, Materials Modification by Electronic Excitation, Cambridge Univ. Press, Cambridge (2001).
[4] F. Weigert, Ann. Phys. **63,** 681 (1920).
[5] T. Tani, Photographic Sensitivity, Oxford Univ. Press, Oxford (1995).
[6] Z. U. Borisova, Glassy Semiconductors, Plenum, New York (1981).
[7] M. A. Popescu, Non-Crystalline Chalcogenides, Kluwer Academic Publishers, Dordrecht, (2000).
[8] K. Tanaka, Bulgarian Chem. Commun. **26,** 450 (1993).
[9] K. Tanaka, J. Appl. Phys. **49,** 6132 (1978).
[10] M. Fernandez-Guasti, E. Haro-Poniatowski, S. Camacho-Lopez, Appl. Opt. **31,** 3453 (1992).
[11] V. Palyok, I.A. Szabo, D.L. Beke, A. Kikineshi, Appl. Phys. A **74,** 683 (2002).
[12] J. Dikova, Tz. Babeva, P. Sharlandjiev, J. Optoelectron. Adv. Mater. **7,** 361 (2005).
[13] H. Hamanaka, Ka. Tanaka, A. Matsuda, S. Iijima, Solid State Commun. **19,** 499 (1976).
[14] H. Hisakuni, K. Tanaka, Appl. Phys. Lett. **65,** 2925 (1994).
[15] H. Hisakuni, K. Tanaka, Opt. Lett. **20,** 958 (1995).
[16] A. Saitoh, T. Gotoh, K. Tanaka, J. Non-Cryst. Solids **299-302,** 983 (2002).
[17] A. Saitoh, K. Tanaka, Appl. Phys. Lett. **83,** 1725 (2003).
[18] S. Ramachandran, S.G. Bishop, J.P. Guo, D.J. Brady, IEEE Photonics Technol. Lett. **8,** 1041 (1996).
[19] K. Tanaka, Phys. Rev. B **57,** 5163 (1998).
[20] H. Hisakuni, K. Tanaka, Science **270,** 974 (1995).
[21] K. Tanaka, C.R. Chimie **5,** 805 (2002).
[22] K. Tanaka, Photo-Induced Metastability in Amorphous Semiconductors, Ed. A.V. Kolobov, Wiley-VCH, (2003) Chap. 5.

[23] J. Gump, I. Finkler, H. Xia, R. Sooryakumar, W. J. Bresser, P. Boolchand, Phys. Rev. Lett. **92,** 245501 (2004).
[24] M.L. Trunov, S.N. Dub, R.S. Shmegera, J. Optoelectron. Adv. Mater. **7,** 619 (2005).
[25] K. Tanaka, J. Non-Cryst. Solids **266-269,** 889 (2000).
[26] K. Shimakawa, N. Yoshida, A. Ganjoo, Y. Kuzukawa, J. Singh, Philos. Mag. Lett. **77,** 153 (1998).
[27] K. Shimakawa, J. Optoelectron. Adv. Mater. **7,** 145 (2005).
[28] E.V. Emelianova, G.J. Adriaenssens, V.I. Arkhipov, Philos. Mag. Lett. **84,** 47 (2004).
[29] V.G. Zhdanov, V.K. Malinovskii, Sov. Tech. Phys. Lett. **3,** 387 (1977).
[30] K. Tanaka, Handbook of Advanced Electronic and Photonic Materials and Devices, Ed. H.S. Nalwa, Academic Press, (2001) Vol. 5, Chap. 4.
[31] V. M. Lyubin, M. L. Klebanov, Photo-Induced Metastability in Amorphous Semiconductors, Ed. A.V. Kolobov, Wiley-VCH, Winheim, (2003) Chap. 6.
[32] H. Fritzsche, J. Non-Cryst. Solids **164/166,** 1169 (1993).
[33] H. Fritzsche, Insulating and Semiconducting Glasses, Ed. P. Boolchand, World Scientific, Singapole, (2000), Chap. 10.
[34] G. Chen, H. Jain, M. Vlcek, S. Khalid, J. Li, D.A. Drabold, S.R. Elliott, Appl. Phys. Lett. **82,** 706 (2003).
[35] K. Tanaka, K. Ishida, N. Yoshida, Phys. Rev. B **54,** 9190 (1996).
[36] A.V. Kolobov, H. Oyanagi, Ka. Tanaka, Phys. Rev. Lett. **87,** 145502 (2001).
[37] K. Ishida, K. Tanaka, Phys. Rev. B **56,** 206 (1997).
[38] V. Lyubin, M. Klebanov, M. Mitkova, T. Petkova, J. Non-Cryst. Solids **227-230,** 739 (1998).
[39] T. Innami, S. Adachi, Phys. Rev. B **60,** 8284 (1999).
[40] P. Krecmer, A.M. Moulin, R.J. Stephenson, T. Rayment, M.E. Welland, S.R. Elliott, Science, **277,** 1799 (1997).
[41] M. Stuchlik, P. Krecmer, S.R. Elliott, Photo-Induced Metastability in Amorphous Semiconductors, Ed. A.V. Kolobov, Wiley-VCH, Winheim, (2003) Chap. 7.
[42] A. Saliminia, T. V. Galstian, A. Villeneuve, Phys. Rev. Lett. **85,** 4112 (2000).
[43] K. E. Asatryan, T. V. Galstian, A. Villeneuve, Phys. Rev. Lett. **94,** 87401 (2005).
[44] Such non-monotonic exposure-time dependence may be a reason why the anisotropic deformation could not be found until 2000. Actually, we had been satisfied with the giant expansion, assuming that this was an ultimate effect! In addition, prominent anisotropic deformations can appear under restricted experimental conditions. For instance, a good condition for observing the anisotropic deformation is a light spot of 5 – 10 μm in diameter and film thickness of ~2 μm. If the film thickness is much greater than the spot size, the deformation is masked by the giant volume expansion. In addition, in focused light exposures, accurate optical alignments are needed, as will be reported elsewhere.
[45] E. Tarnow, A. Antoneli, J. D. Joannopoulos, Phys. Rev. B **34,** 4059, (1986).
[46] K. Tanaka, J. Non-Cryst. Solids **59&60,** 925 (1983).
[47] H. Koseki, A. Odajima, Jpn. J. Appl. Phys. **21,** 424 (1982).
[48] J. Li, D. A. Drabold, Phys. Rev. Lett. **85,** 2785 (2000).
[49] T. Kawaguchi, K. Tanaka, S. R. Elliott, Handbook of Advanced Electronic and Photonic Materials and Devices, Ed. H. S. Nalwa, Academic Press, (2001) Vol. 5, Chap. 3.
[50] T. Wagner, M. Frumar, Photo-Induced Metastability in Amorphous Semiconductors, Ed. A. V. Kolobov, Wiley-VCH, Winheim, (2003) Chap. 10.
[51] K. Tanaka, T. Gotoh, H. Hayakawa, Appl. Phys. Lett. **75,** 2256 (1999).
[52] T. Gotoh, H. Hayakawa, K. Tanaka, J. Non-Cryst. Solids **266-269,** 944 (2000).
[53] T. Gotoh, K. Tanaka, J. Appl. Phys. **89,** 4697 (2001).
[54] T. Gotoh, K. Tanaka, J. Appl. Phys. **89,** 4703 (2001).
[55] M. Ohto, K. Tanaka, J. Non-Cryst. Solids **227-230,** 784 (1998).

[56] M. Ohto, K. Tanaka, J. Appl. Phys. **92,** 5468 (2002).
[57] K. Tanaka, N. Nemoto, H. Nasu, Jpn. J. Appl. Phys. **42,** 6748 (2003).
[58] N. Yoshida, K. Tanaka, J. Non-Cryst. Solids **210,** 119 (1997).
[59] K. Tanaka, N. Yoshida, Y. Yamaoka, Philos. Mag. Lett. **68,** 81 (1993).
[60] N. Yoshida, K. Tanaka, J. Appl. Phys. **78,** 1745 (1995).
[61] K. Tanaka, M. Itoh, N. Yosida, M. Ohto, J. Appl. Phys. **78,** 3895 (1995).